Sensor and Simulation Notes

Note 582

December 22, 2019

Analysis of Stray Capacitances in Compact Marx Generators

Dr. D. V. Giri
Pro-Tech, Wellesley MA
Dept. of ECE, University of New Mexico, Albuquerque, NM
www.dvgiri.com Giri@DVGiri.com

and

Prof. Shubho Banerjee
Dept. of Physics, Rhodes College, Memphis TN
banerjees@rhodes.edu

Abstract

Stray capacitances in switches play a significant role in the functioning of Marx generators. Knowing the dependence of these capacitances on various geometrical parameters is thus very useful in the design phase of these generators. By modeling a switch as two charged electrical conductors embedded in a grounded cylinder we calculate the capacitance between the two spheres and the capacitance between the sphere and the grounded cylinder, in series form. This note is an expanded version our recent paper in the IEEE transactions on Plasma Science [1].

Keywords: electrostatic interaction, conducting spheres, capacitances, Marx generators, grounded cylinder.

Acknowledgement

The authors are thankful to Prof. Jane M. Lehr of Dept. of ECE, University of New Mexico, Albuquerque, NM for suggesting this problem that came up during her research on compact Marx generators. Her student J. Cameron Pouncey provided valuable assistance in the comparison of his numerical solution with the closed-form expressions developed in this paper.

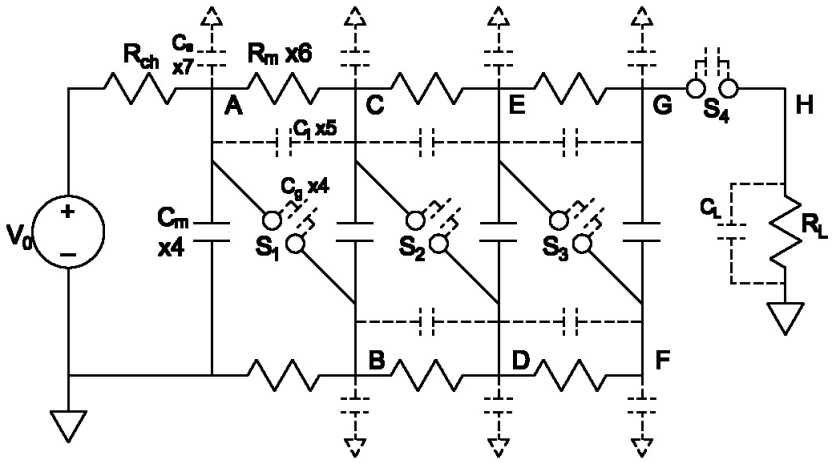

Figure 1: A schematic of the four stage Marx generator showing the stray capacitances S_1, S_2, and S_3 of interest that can adversely impact the performance of the generator.

1 Introduction

Spark-gap switches in high-power transient generators often involve spherical conductors inside a grounded cylinder. One popular example of such a machine is the Marx generator [2] wherein many identical capacitors are charged in parallel from a single DC source and then these charged capacitors are connected in series to multiply the voltage. This process of erecting the voltage is accomplished by a switch between the first two capacitors. Generally speaking, after the first two capacitors are connected in series by the closure of the first switch, the remaining series connections are achieved by over-voltages.

However, the stray capacitances across the switch conductors and the capacitance between one of the switch conductors and the grounded cylindrical tube affect the performance resulting in some erratic behavior in switching. This behavior is more of an issue in compact Marx generators where the capacitances discussed above have an enhanced effect. Figure 1 illustrates the schematic of a 4-stage Marx generator.

The stray capacitances across the Marx switches S_1 to S_3 and the stray capacitances to ground impact the Marx performance significantly especially in compact Marx generators. The erratic behavior happens when the Marx switches do not close in the desired sequence, but close in some random fashion. Builders of compact Marx generators compensate for this lack of knowledge of the strays by experimentally adjusting the Marx parameters till they get decent and predictable performance.

The problem was posed to us by someone who observed this stray capacitance phenomenon and wished to address it analytically. Knowing the stray capacitances results in an informed design for compact Marx generators that can avoid erratic behavior. The switch electrodes represented by the two spheres are of identical radii and we have addressed this geometry. It is possible, but not so useful, to make the radii different. The corresponding electrostatic problem can be formulated as shown in Figure 2.

The three geometrical parameters a, R and H are shown. When the length of the cylinder is large compared to the three geometrical parameters, it is acceptable to consider the cylinder

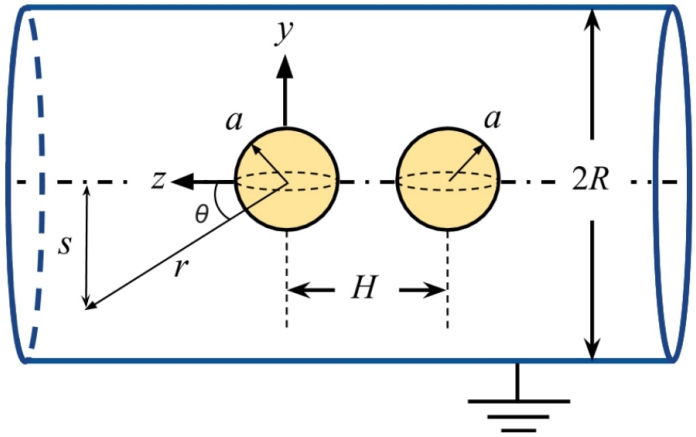

Figure 2: Two spherical electrodes of equal radii a separated by a center-to-center distance H, are held inside an infinitely long grounded cylinder of radius R. The z axis is chosen along the central axis of the cylinder, and the origin is chosen at the center of one of the spheres. The center of the second sphere is at $z = -H$ on the central axis of the cylinder. Any arbitrary location is specified using r, θ coordinates centered on the first sphere. The distance of the location from the central axis is denoted by s.

length to be infinite. It is noted that most of field line perturbations happen around and between the spheres. We seek the capacitance coefficients C_{11} and C_{12} between the spheres in presence of the grounded cylinder. These capacitances can be normalized to the capacitance of the isolated sphere of radius a, given by $C_0 = 4\pi\epsilon_0 a$ where ϵ_0 is the free space permittivity $=1/(36\pi 10^9)$ F/m.

In a recent paper [1] we published the main results of our analysis. In this extended note we have added a new section on the review and extension of the analysis of one sphere in a grounded sphere to include odd multipole terms. Additionally, we have added two new sections on the monopole and quadrupole approximations for the electrostatic potential. Other than these additions we have changed the language in some places for improved clarity and completely rewritten the abstract and summary sections.

2 Motivation and Solution Approach

Our literature search has revealed that a problem of this type was first solved by R. C. Knight [3] in 1935 where he addressed the case of one sphere in a grounded cylinder (see Figure 3). W. R. Smythe [4] offered an alternate solution to the same problem of a charged sphere in a grounded cylinder in 1960. Later Smythe [5] generalized it to a charged spheroid in a grounded cylinder in 1963. Chang and Chang [6] also analyzed this problem in 1967. Furthermore, the electrostatic characteristics of two isolated spheres was considered by many researchers, examples of which are found in [7–9]. However, we have not been able to find a solution to the practical problem of two charged spheres in a grounded cylinder after a thorough literature search.

Of course, it is relatively easy to place the problem on an electrostatic computer program,

of which there are many, and get a quick solution.

This problem was suggested to us by Prof. Jane Lehr of University of New Mexico who was looking for a closed form solution for the capacitances and especially their dependence on various geometrical parameters. The elegant art of analyzing problems analytically seems to be waning in modern times as software routines abound. We were motivated to tackle this problem analytically for three reasons; a) it is somewhat puzzling that such an elegant problem has not been done before and b) our solution clearly demonstrates the dependence the of the capacitances on various geometrical parameters in the problem and c) the analytical results can serve as a test case to check the accuracy of numerical results.

Our approach is straightforward. We extend the solution of Laplace equation of Chang and Chang [6] for one sphere to the present case of two spheres in a grounded cylinder. It is observed that in problems of this type, the choice of coordinates system has a huge impact. Note that we have two spherical conductors inside a cylinder. There are two possible spherical coordinate systems centered on either sphere or cylindrical coordinates. Laplace equation yields Bessel type of solutions in cylindrical and Legendre polynomial solutions in spherical coordinates. We use a spherical coordinate system centered on one of the spheres and develop equations for the other two conductors in the chosen coordinate system.

We write the solution of Laplace equation everywhere in the grounded cylinder and the boundary conditions on the perfectly conducting spheres and the perfectly conducting and infinitely long cylinder are satisfied. We then take the gradient of the potential to get the electric field everywhere. The normal component of the electric field on the spheres is proportional to the charge distribution ($\mathrm{C/m^2}$) written as a multipole expansion. Integrating the charge distribution on the spheres yields the total charge on the sphere. Knowing the total charge and voltages on the sphere finally leads to the capacitance estimates which is the goal of the problem.

It is noted that the multipole expansion of the charge distribution is an alternative to the theory of successive and infinite images of one spherical charge in the other sphere. Due to the presence of the grounded cylinder solving the Laplace equation is the simpler approach for this problem.

3 Review and generalization of the Chang and Chang formulation

In this section we review the Chang and Chang (CC) formulation of the problem of one sphere inside a grounded cylinder. See Figure 3 for the geometry of the set up. We make minor notation changes to CC in order to make the dimensional dependence of the potential on the cylinder radius R, more explicit; CC set $R = 1$ in their paper. The formulation begins by creating one solution that satisfies the Laplace equation inside the cylinder

$$\varphi = \frac{1}{r} - \frac{1}{R}\int_0^\infty f(\lambda) I_0(\tfrac{\lambda s}{R}) \cos\tfrac{\lambda z}{R}\, d\lambda, \tag{1}$$

where I_0 is the modified Bessel function of the first kind, λ is a dimensionless integration variable, and f is any function. The first term in φ is from a charge monopole, and the second

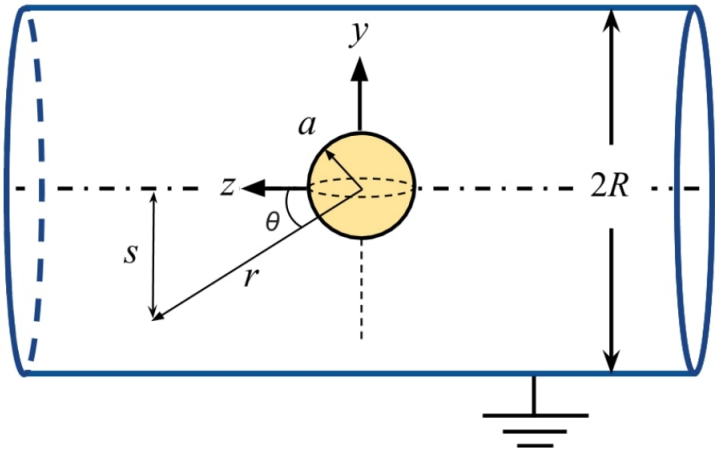

Figure 3: A spherical electrode of radius a held inside an infinitely long grounded cylinder of radius R. The z axis is chosen along the central axis of the cylinder, and the origin is chosen at the center of the sphere. Any arbitrary location is specified using polar coordinates (r, θ) centered on the sphere. The distance of the location from the central axis is denoted by s. This set up is a simpler version of that discussed in Fig. 2 without the second sphere.

term is for the interior of a cylinder of radius R. To impose proper boundary conditions on the cylinder in the presence of the monopole term, CC note that it is possible to write the monopole term in cylindrical form as

$$\frac{1}{r} = \frac{2}{\pi R} \int_0^\infty K_0(\tfrac{\lambda s}{R}) \cos \tfrac{\lambda z}{R} \; d\lambda, \tag{2}$$

where K_0 is the modified Bessel function of the second kind. The function f in Equation (1) is then chosen in the following manner so that $\varphi = 0$ when $s = R$ for any z:

$$\varphi = \frac{1}{r} - \frac{2}{\pi R} \int_0^\infty \frac{K_0(\lambda)}{I_0(\lambda)} I_0(\tfrac{\lambda s}{R}) \cos \tfrac{\lambda z}{R} \; d\lambda. \tag{3}$$

This φ is the solution to the Laplace equation for a monopole located at the origin inside the grounded cylinder.

Since CC only consider a sphere with symmetric charge distributions with respect to z, they create higher order multipolar solutions by taking even numbered derivatives of φ with respect to z

$$\Phi_{2n} = \frac{1}{(2n)!} \frac{\partial^{2n} \varphi}{\partial z^{2n}} = \frac{P_{2n}(\cos\theta)}{r^{2n+1}} + \frac{(-1)^{n+1}}{(2n)!} \frac{2}{\pi R^{2n+1}} \int_0^\infty \frac{\lambda^{2n} K_0(\lambda)}{I_0(\lambda)} I_0(\tfrac{\lambda s}{R}) \cos \tfrac{\lambda z}{R} \; d\lambda. \tag{4}$$

By construction, Φ_{2n} is the solution for the $2n^{\text{th}}$ multipole placed at the origin inside the grounded cylinder. However, the integral in the second term, due to the induced charges on the cylinder, hides important dependencies on r and θ.

To create a multipolar decomposition of the potential due to the induced charges on the cylinder, CC in their Appendix show that

$$I_0(\tfrac{\lambda s}{R})\cos\tfrac{\lambda z}{R} = \sum_{m=0}^{\infty}(-1)^m \frac{\lambda^{2m}}{(2m)!}\frac{r^{2m}}{R^{2m}}P_{2m}(\cos\theta). \tag{5}$$

Substituting this result back into the integral above gives

$$\Phi_{2n}(r,\theta) = \frac{P_{2n}(\cos\theta)}{r^{2n+1}} - \sum_{m=0}^{\infty} C_{nm}\frac{r^{2m}}{R^{2n+2m+1}}P_{2m}(\cos\theta) \tag{6}$$

where

$$C_{nm} = \frac{2}{\pi}\frac{(-1)^{n+m}}{(2n)!(2m)!}\int_0^{\infty}\frac{\lambda^{2(n+m)}K_0(\lambda)}{I_0(\lambda)}d\lambda \tag{7}$$

are dimensionless coefficients that can be calculated and tabulated using numerical integration. The general solution for potentials symmetric in z and grounded at $s = R$ can then be written as

$$V_{\text{even}}(r,\theta) = \sum_{n=0}^{\infty} A_{2n}\left[\frac{P_{2n}(\cos\theta)}{r^{2n+1}} - \sum_{m=0}^{\infty}\frac{C_{nm}r^{2m}P_{2m}(\cos\theta)}{R^{2n+2m+1}}\right], \tag{8}$$

where A_{2n} is the strength of the $2n^{\text{th}}$ multipole moment.

While this formulation is sufficient for the CC case where there is one conducting sphere inside the grounded cylinder, it fails for cases when the potential is asymmetric in z. For example, the potential does not describe the simple case of a dipole placed at the origin inside the cylinder. Generalization of the CC formulation to include odd multipoles is therefore needed to describe potentials that lack even symmetry in z.

To develop the potential for odd multipoles, we differentiate Equation (3) $2l+1$ times with respect to z to get

$$\Phi_{2l+1} = \frac{1}{(2l+1)!}\frac{\partial^{2l+1}\varphi}{\partial z^{2l+1}} = \frac{P_{2l+1}(\cos\theta)}{r^{2l+2}} + \frac{(-1)^{l+1}}{(2l+1)!}\frac{2}{\pi R^{2l+2}}\int_0^{\infty}\frac{\lambda^{2l+1}K_0(\lambda)}{I_0(\lambda)}I_0(\tfrac{\lambda s}{R})\sin\tfrac{\lambda z}{R}\ d\lambda. \tag{9}$$

Following the same technique as outlined in the CC Appendix we get

$$I_0(\tfrac{\lambda s}{R})\sin\tfrac{\lambda z}{R} = \sum_{k=0}^{\infty}(-1)^k\frac{\lambda^{2k+1}}{(2k+1)!}\frac{r^{2k+1}}{R^{2k+1}}P_{2k+1}(\cos\theta). \tag{10}$$

Substituting this result back into the integral above gives

$$\Phi_{2l+1}(r,\theta) = \frac{P_{2l+1}(\cos\theta)}{r^{2l+2}} - \sum_{k=0}^{\infty} D_{lk}\frac{r^{2k+1}}{R^{2l+2k+2}}P_{2l+1}(\cos\theta) \tag{11}$$

where

$$D_{lk} = \frac{2}{\pi}\frac{(-1)^{l+k}}{(2l+1)!(2k+1)!}\int_0^\infty \frac{\lambda^{2(l+k+1)}K_0(\lambda)}{I_0(\lambda)}d\lambda. \tag{12}$$

The general solution for potentials anti-symmetric in z and grounded at $s = R$ can then be written as

$$V_{\text{odd}}(r,\theta) = \sum_{l=0}^{\infty} A_{2l+1}\left[\frac{P_{2l+1}(\cos\theta)}{r^{2l+2}} - \sum_{k=0}^{\infty}\frac{D_{lk}r^{2k+1}P_{2k+1}(\cos\theta)}{R^{2l+2k+3}}\right]. \tag{13}$$

The complete multipole expansion for the potential inside the grounded cylinder is the sum of the symmetric and anti-symmetric potentials

$$\begin{aligned} V(r,\theta) = &\sum_{n=0}^{\infty} A_{2n}\left[\frac{P_{2n}(\cos\theta)}{r^{2n+1}} - \sum_{m=0}^{\infty}\frac{C_{nm}r^{2m}P_{2m}(\cos\theta)}{R^{2n+2m+1}}\right] \\ &+ \sum_{l=0}^{\infty} A_{2l+1}\left[\frac{P_{2l+1}(\cos\theta)}{r^{2l+2}} - \sum_{k=0}^{\infty}\frac{D_{lk}r^{2k+1}P_{2k+1}(\cos\theta)}{R^{2l+2k+3}}\right]. \end{aligned} \tag{14}$$

This potential is valid for any charge distribution centered at the origin as long as r is outside the distribution and $r < R$.

In the case of CC, a single sphere with radius a at the origin held at a constant voltage $V = 1$, the potential in the region $a < r < R$ is specified using the additional boundary condition $V(a,\theta) = 1$. Since the potential is symmetric in z, we have $A_{2l+1} = 0$ for all l. The coefficients A_{2n} can be determined approximately by terminating the series at some finite $n+1 = N$ number of multipoles and then imposing the boundary conditions on the sphere at $N+1$ different points. The capacitance of the sphere is calculated using $C = 4\pi\epsilon_0 A_0$, where the monopole term A_0 is a measure of the charge on the sphere.

4 General potential formulation for two spheres

We now use this generalized potential fortified with odd terms to create the general result for two spheres. The main idea of our approach below is to use the principle of superposition. The sum of two multipole expansions, one centered at each spheres satisfies the Laplace equation in the region outside the two spheres and inside the cylinder.

4.1 The geometry of the problem

Both spheres are of the same radius a. The first sphere is at the origin and r, θ are the coordinates of any point from the center of this sphere. The center of the second sphere is at a height $z = -2h = -H$ from the origin.

The coordinates of any point r, θ as measured from the second sphere are given by

$$r_b = \sqrt{r^2 + H^2 + 2rH\cos\theta} \tag{15}$$

$$\theta_b = \cos^{-1}\left(\frac{H + r\cos\theta}{r_b}\right). \tag{16}$$

To obtain the required capacitances, we need to solve both symmetric and anti-symmetric problems.

4.2 The symmetric +V/+V case

For the symmetric case we may assume that both spheres are held at potential $V = +1$ volt. The general form of the potential for this case can be written as

$$V_+(r,\theta) = V(r,\theta) + V'(r_b,\theta_b). \tag{17}$$

where the coefficients for $V'(r_b,\theta_b)$ are $A^{+\prime}_{2n} = A^+_{2n}$ and $A^{+\prime}_{2l+1} = -A^+_{2l+1}$ to make the potential top-down symmetric.

The boundary conditions to determine the constants A^+_{2n} and A^+_{2l+1} are

$$V_+(a,\theta) = 1, \tag{18}$$

for all angles θ. This yields the infinite equations needed to be solved to uniquely determine all the multipole coefficients. It is not clear if a general closed-form solution for this problem exists.

However, we may construct approximate solutions by limiting ourselves to a finite number of multipole coefficients and assuming that the contribution from the higher order multipole terms is negligibly small. That is, let only $A^+_0, A^+_1, ..., A^+_{N-1}$ be nonzero, where N is the number of nonzero multipoles and all higher multipoles be zero.

The equations that determine these N multipole moments can be obtained by fixing the potential at N evenly spaced points on the sphere

$$\mathbf{M}^+\mathbf{A}^+ = \mathbf{1} \tag{19}$$

where $\mathbf{A}^+$ and $\mathbf{1}$ are $N \times 1$ column vectors with entries $A^+_0, A^+_1, ..., A^+_{N-1}$ and $1, 1, ..., 1$ respectively and the $N \times N$ matrix $\mathbf{M}^+$ has the odd columns

$$\begin{aligned} M^+_{p+1,2n+1} = \frac{1}{a^{2n+1}}\Bigg[& P_{2n}(\cos\tfrac{p\pi}{N-1}) + \frac{a^{2n+1}}{X_p^{2n+1}} P_{2n}(\cos\theta_{bp}) \\ & - \sum_{m=0}^{\infty} \frac{C_{nm}\left\{a^{2n+1}X_p^{2m}P_{2m}(\cos\theta_{bp}) + a^{2n+2m+1}P_{2m}(\cos\tfrac{p\pi}{N-1})\right\}}{R^{2n+2m+1}}\Bigg] \end{aligned} \tag{20}$$

and the even columns

$$\begin{aligned} M^+_{p+1,2l+2} = \frac{1}{a^{2l+2}}\Bigg[& P_{2l+1}(\cos\tfrac{p\pi}{N-1}) - \frac{a^{2l+2}}{X_p^{2l+2}} P_{2l+1}(\cos\theta_{bp}) \\ & + \sum_{k=0}^{\infty} \frac{D_{lk}\left\{a^{2l+2}X_p^{2k+1}P_{2k+1}(\cos\theta_{bp}) - a^{2l+2k+3}P_{2k+1}(\cos\tfrac{p\pi}{N-1})\right\}}{R^{2l+2k+3}}\Bigg] \end{aligned} \tag{21}$$

with $0 \le 2n \le N-1$ and $0 \le 2l \le N-2$. The integer $0 \le p \le N-1$ generates the N boundary conditions on the first sphere at the coordinates $X_p = \sqrt{a^2 + H^2 + 2aH\cos\frac{p\pi}{N-1}}$ and $\cos\theta_{bp} = (H + a\cos\frac{p\pi}{N-1})/X_p$ from the center of the second sphere. The multipole values needed to satisfy the boundary conditions can be obtained by multiplying Equation (19) by the inverse of $\mathbf{M}^+$.

4.3 The anti-symmetric +V/-V case

For the anti-symmetric case the second sphere is held at potential $V = -1$ volt instead. The general form of the potential for this case can be written as

$$V_-(r,\theta) = V(r,\theta) + V'(r_b,\theta_b), \tag{22}$$

where the coefficients of V' are $A_{2n}^{-\prime} = -A_{2n}^-$ and $A_{2l+1}^{-\prime} = A_{2l+1}^-$ to make the potential anti-symmetric.

The boundary conditions to determine the constants A_{2n}^- and A_{2l+1}^- are

$$V_-(a,\theta) = 1, \tag{23}$$

for all angles θ. This yields the infinite equations needed to be solved to uniquely determine all the multipole coefficients. It is not clear if a general closed-form solution for this problem exists. Similar to symmetric case, we may construct approximate solutions by limiting ourselves to a finite number of multipole coefficients and assuming that the contribution from the higher order multipole terms is negligibly small. That is, let only $A_0^-, A_1^-, ..., A_{N-1}^-$ be nonzero, where N is the number of nonzero multipoles, and all higher multipoles be zero.

The equations that determine these N multipole coefficients are can be written in the matrix form

$$\mathbf{M}^-\mathbf{A}^- = \mathbf{1} \tag{24}$$

where $\mathbf{A}^-$ and $\mathbf{1}$ are $N \times 1$ column vectors with entries $A_0^-, A_1^-, ..., A_7^-$ and $1, 1, ..., 1$ respectively and the $N \times N$ matrix $\mathbf{M}^-$ has the odd columns

$$\begin{aligned} M_{p+1,2n+1}^- = \frac{1}{a^{2n+1}}\Bigg[& P_{2n}(\cos\tfrac{p\pi}{N-1}) - \frac{a^{2n+1}}{X_p^{2n+1}} P_{2n}(\cos\theta_{bp}) \\ & + \sum_{m=0}^{\infty} \frac{C_{nm}\left\{a^{2n+1}X_p^{2m}P_{2m}(\cos\theta_{bp}) - a^{2n+2m+1}P_{2m}(\cos\tfrac{p\pi}{N-1})\right\}}{R^{2n+2m+1}}\Bigg] \end{aligned} \tag{25}$$

and the even columns

$$\begin{aligned} M_{p+1,2l+2}^- = \frac{1}{a^{2l+2}}\Bigg[& P_{2l+1}(\cos\tfrac{p\pi}{N-1}) + \frac{a^{2l+2}}{X_p^{2l+2}} P_{2l+1}(\cos\theta_{bp}) \\ & - \sum_{k=0}^{\infty} \frac{D_{lk}\left\{a^{2l+2}X_p^{2k+1}P_{2k+1}(\cos\theta_{bp}) + a^{2l+2k+3}P_{2k+1}(\cos\tfrac{p\pi}{N-1})\right\}}{R^{2l+2k+3}}\Bigg] \end{aligned} \tag{26}$$

The multipole values needed to satisfy the boundary conditions can be obtained by multiplying Equation (24) by the inverse of $\mathbf{M}^-$.

Note that the formalism presented in this section is for any arbitrarily large number N of multipole terms. More and more multipole terms can be included until the desired threshold for convergence is achieved. In principle, an analytical solution for any finite N can be achieved by calculating the inverse of the $\mathbf{M}^{\pm}$ matrices. The errors in voltage readings on the spheres for the N term multipole approximation are of order $(a/H)^{N+1}$. Empirically, the errors lie within two times this factor.

5 Monopole approximation

It is instructive to solve the symmetric and antisymmetric problems exactly for some small N values to explicitly determine the dependence of the multipole coefficients on the geometrical parameters of the system.

The simplest is the $N = 1$ case where only the monopole coefficient is nonzero. In this case the general formulation above yields the angle undefined $p\pi/(N-1) = 0/0$. We arbitrarily choose that point to be at the top of the sphere for algebraic simplicity.

For the symmetric case we have the boundary condition

$$V_+(a,0) = A_0^+ \left[\frac{1}{a} + \frac{1}{X_0} - \sum_{m=0}^{\infty} \frac{C_{0m}(a^{2m} + X_0^{2m}) P_{2m}(1)}{R^{2m+1}} \right] = 1, \tag{27}$$

where $X_0 = H + a$. Solving for A_0^+ gives

$$\frac{A_0^+}{a} = \left[1 + \frac{a}{X_0} - \sum_{m=0}^{\infty} \frac{C_{0m}(aX_0^{2m} + a^{2m+1})}{R^{2m+1}} \right]^{-1}. \tag{28}$$

We may include as many C_{0m} terms here as needed to get convergence to the final answer. More m terms will be needed for larger a or larger H values.

For the anti-symmetric case we get the boundary condition

$$V_-(a,0) = A_0^- \left[\frac{1}{a} - \frac{1}{X_0} - \sum_{m=0}^{\infty} \frac{C_{0m}(a^{2m} - X_0^{2m}) P_{2m}(1)}{R^{2m+1}} \right] = 1, \tag{29}$$

Solving For A_0^- gives

$$\frac{A_0^-}{a} = \left[1 - \frac{a}{X_0} + \sum_{m=0}^{\infty} \frac{C_{0m}(aX_0^{2m} - a^{2m+1})}{R^{2m+1}} \right]^{-1}. \tag{30}$$

We may include as many C_{0m} terms here as needed to get convergence to the final answer. More m terms will be needed for larger a or larger H values. The errors in the monopole approximation are about two times $(a/H)^2$ and so it may be used as long as $a << H$.

6 Dipole approximation

As another example of the formalism presented in Section 4 we calculate the details of the dipole approximation ($N = 2$), i.e., we assume that both monopole and dipole moments are nonzero. The dipole approximation does not yield very good results (as seen in later sections) but it is algebraically simple to show on paper. Higher order multipole calculations can be carried out in a similar manner as below but with the help of a computer. In the next section we present approximate but accurate expressions for the quadrupole approximation.

6.1 The symmetric +V/+V case

In this case the equations that determine these two coefficients, A_0^+ and A_1^+, are

$$V_+(a,0) = 1 = \frac{A_0^+}{a}\left[1 + \frac{a}{X_0} - \sum_{m=0}^{\infty} \frac{C_{0m}(aX_0^{2m} + a^{2m+1})}{R^{2m+1}}\right] + \frac{A_1^+}{a^2}\left[1 - \frac{a^2}{X_0^2} + \sum_{k=0}^{\infty} \frac{D_{0k}(a^2X_0^{2k+1} - a^{2k+3})}{R^{2k+3}}\right], \quad (31)$$

and

$$V_+(a,\pi) = 1 = \frac{A_0^+}{a}\left[1 + \frac{a}{X_1} - \sum_{m=0}^{\infty} \frac{C_{0m}(aX_1^{2m} + a^{2m+1})}{R^{2m+1}}\right] - \frac{A_1^+}{a^2}\left[1 + \frac{a^2}{X_1^2} - \sum_{k=0}^{\infty} \frac{D_{0k}(a^2X_1^{2k+1} + a^{2k+3})}{R^{2k+3}}\right], \quad (32)$$

where $X_0 = H + a$ and $X_1 = H - a$. We may write the two boundary conditions above in the matrix form

$$\begin{pmatrix} \alpha^+ & \beta^+ \\ \gamma^+ & \delta^+ \end{pmatrix} \begin{pmatrix} A_0^+ \\ A_1^+ \end{pmatrix} = \begin{pmatrix} 1 \\ 1 \end{pmatrix} \quad (33)$$

where α^+, γ^+ are the two coefficients of A_0^+ and β^+, δ^+ are the corresponding coefficients of A_1^+. Solving for A_0^+ and A_1^+ gives

$$\begin{pmatrix} A_0^+ \\ A_1^+ \end{pmatrix} = \frac{1}{\alpha^+\delta^+ - \beta^+\gamma^+} \begin{pmatrix} \delta^+ & -\beta^+ \\ -\gamma^+ & \alpha^+ \end{pmatrix} \begin{pmatrix} 1 \\ 1 \end{pmatrix} \quad (34)$$

which can be written as

$$A_0^+ = \frac{\delta^+ - \beta^+}{\alpha^+\delta^+ - \beta^+\gamma^+} \quad \text{and} \quad A_1^+ = \frac{\alpha^+ - \gamma^+}{\alpha^+\delta^+ - \beta^+\gamma^+}. \quad (35)$$

[t] In Figure 4, we plot the potential on the surface of the first sphere as a function of the angle for the parameters $a/R = 0.1$ and $H/R = 0.5$. In this dipole approximation, the potential is exactly 1 at two points on the sphere and the overall deviation from 1 is less than 1.2%. For comparison, plots from quadrupole and octupole cases are also included to show that the result converges. The deviations in the quadrupole and octupole plots are 0.2% and 0.03% respectively. At $\theta = 0, \pi$ the dipole potential is exactly 1 because A_0^+ and A_1^+ are derived using those conditions.

6.2 The anti-symmetric +V/-V case

For the anti-symmetric potential case, the boundary conditions that determine the monopole and dipole moments A_0^- and A_1^- are

$$V_-(a,0) = 1 = \frac{A_0^-}{a}\left[1 - \frac{a}{X_0} + \sum_{m=0}^{\infty} \frac{C_{0m}(aX_0^{2m} - a^{2m+1})}{R^{2m+1}}\right] + \frac{A_1^-}{a^2}\left[1 + \frac{a^2}{X_0^2} - \sum_{k=0}^{\infty} \frac{D_{0k}(a^2X_0^{2k+1} + a^{2k+3})}{R^{2k+3}}\right], \quad (36)$$

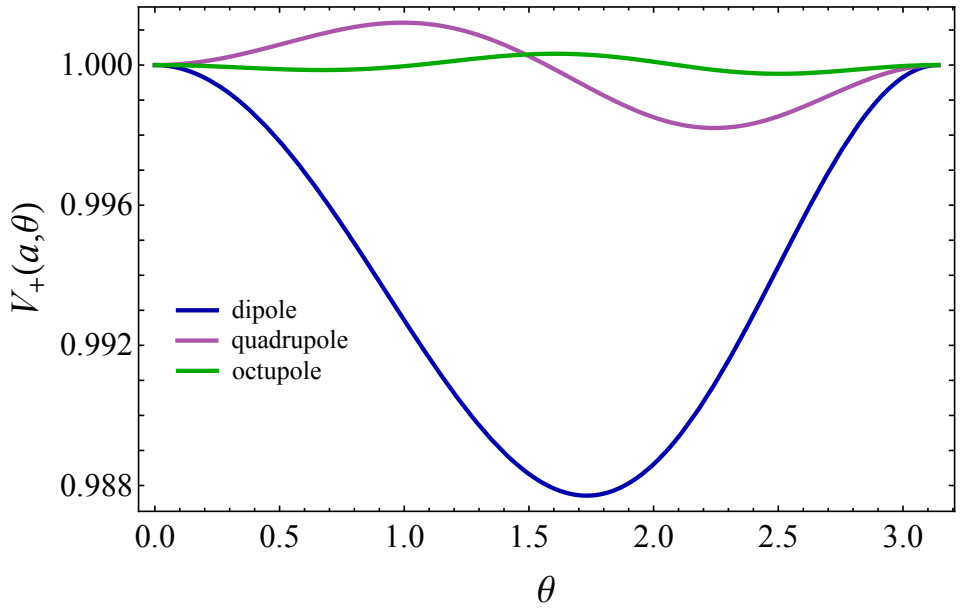

Figure 4: The dipole approximation potential for the first sphere in the $+V/+V$ case is plotted versus the angle for the case $a/R = 0.1$ and $H/R = 0.5$. Also plotted are the potentials from the quadrupole and octupole approximations. The deviations from $V = 1$ decrease as higher multipoles terms are included in the potential.

and

$$V_-(a,\pi) = 1 = \frac{A_0^-}{a}\left[1 - \frac{a}{X_1} + \sum_{m=0}^{\infty} \frac{C_{0m}(aX_1^{2m} - a^{2m+1})}{R^{2m+1}}\right] - \frac{A_1^-}{a^2}\left[1 - \frac{a^2}{X_1^2} + \sum_{k=0}^{\infty} \frac{D_{0k}(a^2X_1^{2k+1} - a^{2k+3})}{R^{2k+3}}\right]. \quad (37)$$

Solving for A_0^- and A_1^- in a similar manner as the symmetric case gives

$$A_0^- = \frac{\delta^- - \beta^-}{\alpha^-\delta^- - \beta^-\gamma^-} \quad \text{and} \quad A_1^- = \frac{\alpha^- - \gamma^-}{\alpha^-\delta^- - \beta^-\gamma^-}, \quad (38)$$

where α^-, γ^- are the coefficients of A_0^- and β^-, δ^- are the corresponding coefficients of A_1^-.

In Figure 5, we plot the potential on the surface of first sphere as a function of the angle for the parameters $a/R = 0.1$ and $H/R = 0.5$. In this dipole approximation, the overall deviation from $V = 1$ is less 1.6%. The deviations for the quadrupole and octupole approximations are less than 0.23% and 0.04% respectively.

7 Quadrupole Approximation

For the quadrupole approximation ($N = 3$) we impose three boundary conditions on the sphere at $\theta = 0, \pi/2$, and π. The solutions to the three multipole moments are obtained by inverting

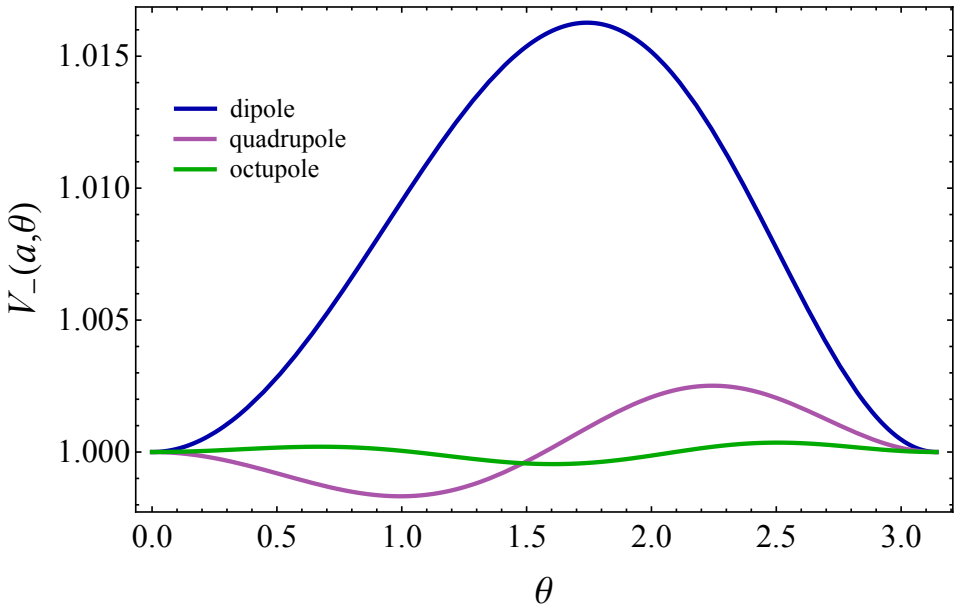

Figure 5: The dipole approximation potential for the first sphere in the $+V/-V$ case is plotted versus the angle for the case $a/R = 0.1$ and $H/R = 0.5$. Also plotted are the potentials from the quadrupole and octupole approximations. The deviations from $V = 1$ decrease as higher multipoles terms are included in the potential.

a 3×3 matrix as discussed earlier. The actual expressions when written in algeraic form are a long and messy and provide little additional insight. However, we may expand the solutions to small powers in (a/H) and keep terms that are consistent with our main approximation of neglecting octupole and higher terms.

For the symmetric case expanding the solutions to order $(a/H)^4$ gives the following approximate but relatively simple form. Here only C_{00}, C_{01}, D_{00} are used, and some higher powers of (H/R) with small coefficients are neglected.

$$\begin{aligned}\frac{A_0^+}{a} \approx 1 &- \frac{a}{H}\left[1 - 1.74138\frac{H}{R} + 0.205911\frac{H^2}{R^2}\right] \\ &+ \frac{a^2}{H^2}\left[1 - 3.48276\frac{H}{R} + 3.03241\frac{H^2}{R^2} + 0.411822\frac{H^3}{R^3} - 0.71714\frac{H^4}{R^4}\right] \\ &- \frac{a^3}{H^3}\left[1 - 5.22414\frac{H}{R} + 9.09722\frac{H^2}{R^2} - 4.66284\frac{H^3}{R^3} - 2.15142\frac{H^4}{R^4} + 1.87322\frac{H^5}{R^5}\right] \\ &+ \frac{a^4}{H^4}\left[2 - 6.96552\frac{H}{R} + 18.1944\frac{H^2}{R^2} - 21.1223\frac{H^3}{R^3} + 4.89264\frac{H^4}{R^4} + 7.49288\frac{H^5}{R^5}\right]\end{aligned} \tag{39}$$

$$\begin{aligned}\frac{A_1^+}{a^2} \approx &\frac{a^2}{H^2}\left[1 - 0.411822\frac{H^3}{R^3}\right] - \frac{a^3}{H^3}\left[1 - 1.74138\frac{H}{R} - 0.205911\frac{H^3}{R^3} + 0.71714\frac{H^4}{R^4}\right] \\ &+ \frac{a^4}{H^4}\left[2 - 3.48276\frac{H}{R} + 3.03241\frac{H^2}{R^2} + 0.71714\frac{H^4}{R^4} - 1.24881\frac{H^5}{R^5}\right]\end{aligned} \tag{40}$$

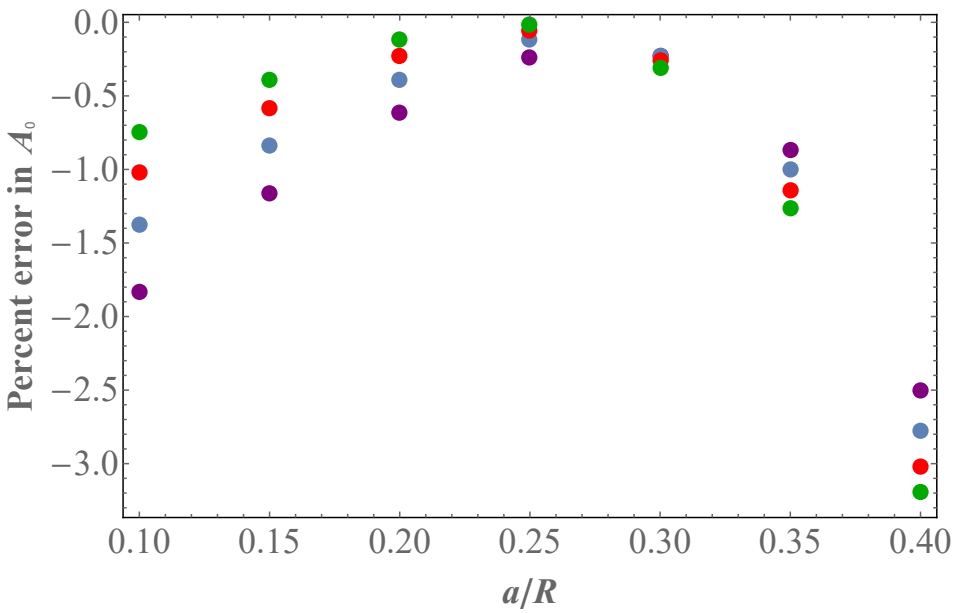

Figure 6: The percent error (remainder) in A_0^+ is plotted versus a/R for $a/H = 0.44$ (purple), 0.42 (blue), 0.40 (red), and 0.38 (green). Exact A_0^+ is calculated using 8 multipole terms $(A_0^+, ..., A_7^+)$ and $m = k = 10$ cylinder terms. Negative remainder indicates that Equation (39) overestimates the monopole term.

$$\frac{A_2^+}{a^3} \approx -\frac{a^3}{H^3}\left[1 + 0.41182\frac{H^3}{R^3}\right] + \frac{a^4}{H^4}\left[1 - 1.74138\frac{H}{R} + 0.617734\frac{H^3}{R^3} - 0.71714\frac{H^4}{R^4} + 0.0848\frac{H^6}{R^6}\right]. \tag{41}$$

In Figure 6 we have plotted the error in the A_0^+ coefficient as a function on the geometrical parameter a/R for some fixed values of a/H.

For including the quadrupole moment we have three boundary conditions on the sphere. Expanding the solutions to order a^6 gives the following approximate form. Only C_{00}, C_{01}, D_{00} are used, some higher powers of (H/R) with small coefficients are neglected.

$$\begin{aligned}\frac{A_0^-}{a} \approx 1 &+ \frac{a}{H}\left[1 + 0.205911\frac{H^3}{R^3}\right] + \frac{a^2}{H^2}\left[1 + 0.411822\frac{H^3}{R^3}\right] + \frac{a^3}{H^3}\left[1 + 0.617734\frac{H^3}{R^3}\right] \\ &+ \frac{a^4}{H^4}\left[2 + 0.423994\frac{H^6}{R^6}\right] + \frac{a^5}{H^5}\left[\frac{43}{12} - 0.205911\frac{H^3}{R^3} + 0.423994\frac{H^6}{R^6}\right] \\ &+ \frac{a^6}{H^6}\left[\frac{43}{6} - 0.329428\frac{H^5}{R^5} + 0.254397\frac{H^6}{R^6} + 0.279377\frac{H^9}{R^9}\right],\end{aligned} \tag{42}$$

$$\begin{aligned}\frac{A_1^-}{a^2} \approx &- \frac{a^2}{H^2}\left[1 - 0.411822\frac{H^3}{R^3}\right] - \frac{a^3}{H^3}\left[1 - 0.205911\frac{H^3}{R^3}\right] - 2\frac{a^4}{H^4} \\ &- \frac{a^5}{H^5}\left[4 + 0.411822\frac{H^3}{R^3} - 0.466394\frac{H^6}{R^6}\right] - \frac{a^6}{H^6}\left[6 - 0.209533\frac{H^9}{R^9}\right],\end{aligned} \tag{43}$$

and

$$\frac{A_2^-}{a^3} \approx \frac{a^3}{H^3} + \frac{a^4}{H^4}\left[1 + 0.205911\frac{H^3}{R^3}\right] + \frac{a^5}{H^5}\left[\frac{17}{12} + 0.411822\frac{H^3}{R^3}\right] + \frac{a^6}{H^6}\left[\frac{53}{12} - 0.531937\frac{H^3}{R^3}\right]. \tag{44}$$

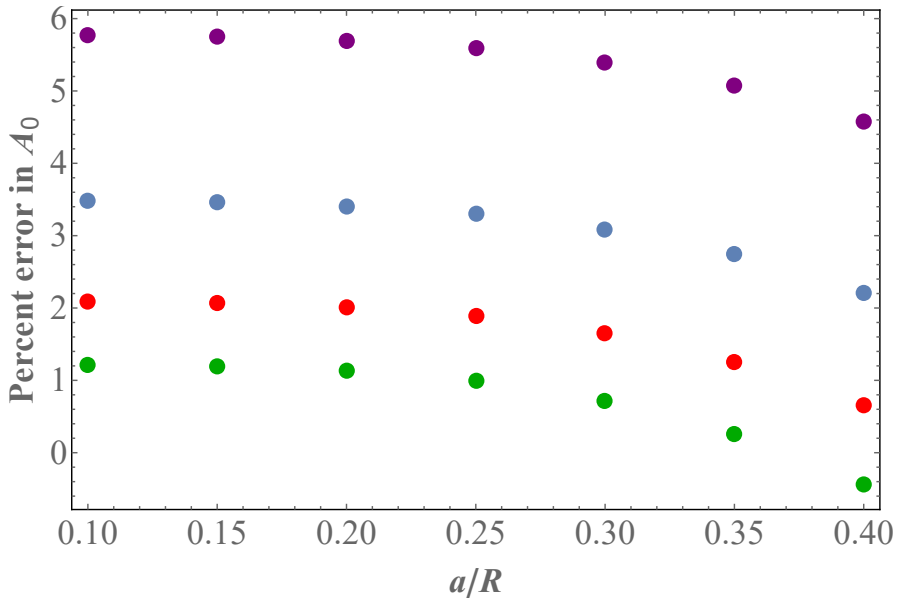

Figure 7: The percent error (remainder) in A_0^- is plotted versus a/R for $a/H = 0.44$ (purple), 0.42 (blue), 0.40 (red), and 0.38 (green). Exact A_0^- is calculated using 8 multipole terms $(A_0^-, ..., A_7^-)$ and $m = k = 10$ cylinder terms. Positive remainder indicates that Equation (42) underestimates the monopole term.

In Figure 7 we have plotted the error in the A_0^- coefficient as a function on the geometrical parameter a/R for some fixed values of a/H.

The octupole ($N = 4$) case is plotted in Figure 5 but not presented here due to its algebraic complexity. In general, it is simpler to calculate the multipolar coefficients for fixed numerical values of the parameters rather than obtaining symbolic solutions.

8 Capacitance calculation

The capacitance coefficients are simply related to the charges on the spheres for specific choice of voltages on the sphere. If both spheres are held at +1 volt then the charge on each sphere is

$$C_+ = C_{11} + C_{12}, \tag{45}$$

and if one sphere is held at 1 volt and the other sphere is held at -1 volt then the charge on the first sphere is

$$C_- = C_{11} - C_{12}. \tag{46}$$

The coefficients C_+ and C_- can be calculated from the solution to Laplace's equation for $V_+(r,\theta)$ and $V_-(r,\theta)$ in the following manner. The charge density on the first sphere is given by

$$\sigma_\pm(\theta) = -\epsilon_0 \left.\frac{\partial V_\pm(r,\theta)}{\partial r}\right|_{r=a}, \tag{47}$$

where ϵ_0 is the permittivity of free space. The capacitance coefficients can be calculated by integrating the charge density over the surface of the sphere

$$C_{\pm} = \int_0^{2\pi} \int_0^{\pi} \sigma_{\pm}(\theta)\, a^2 \sin\theta \, d\theta \, d\phi = 2\pi a^2 \int_0^{\pi} \sigma_{\pm}(\theta)\, \sin\theta \, d\theta. \tag{48}$$

Since the dipole and higher order multipoles carry zero net charge, the charge on the sphere is given by the monopole term in the voltage. This result is confirmed by carrying out a careful calculation of Equation (48) as well. Therefore, we have

$$\frac{C_{\pm}}{4\pi\epsilon_0 a} = \frac{A_0^{\pm}}{a}, \tag{49}$$

where A_0^+, A_0^- are the monopole coefficients from the +V/+V and +V/-V cases respectively. From the above calculation we get

$$\frac{C_{11}}{4\pi\epsilon_0 a} = \frac{1}{2}\left[\frac{C_+ + C_-}{4\pi\epsilon_0 a}\right] = \frac{1}{2}\left[\frac{A_0^+ + A_0^-}{a}\right] \tag{50}$$

and

$$\frac{C_{12}}{4\pi\epsilon_0 a} = \frac{1}{2}\left[\frac{C_+ - C_-}{4\pi\epsilon_0 a}\right] = \frac{1}{2}\left[\frac{A_0^+ - A_0^-}{a}\right]. \tag{51}$$

In previous sections we calculated closed-form expressions for the monopole term $A_0^{\pm}$ in several (monopole, dipole, quadrupole etc.) approximations. By substituting those expressions in the two equations above we generate the following plots in Figures 8-11. The best analytical results (red curve) in these plots are computed by using 8 multipole terms (A_0, ..., A_7) and $m = k = 10$ cylinder terms. Also plotted are simulation results (brown dots) discussed in the next section.

These Figures 8-11 show that for small sphere size $a/R = 0.1$, the quadrupole approximation gives excellent results. However, when the sphere size is larger $a/R = 0.33$, $N = 8$ multipoles are needed for good agreement with the simulation results. A large sphere size reduces the distance between the two spheres and the distance from the spheres to the cylinder. This reduction of distance causes a greater polarization of charge on the spheres. Thus more multipole terms are needed to mimic this polarization of charge on the spheres.

9 Comparison of numerical and analytical solutions

The computation of voltages and capacitances from analytical expressions developed in this paper were compared to a numerical simulation using the commercial CST code.

As seen in Figures 8-11 in Section 8, the capacitance obtained from CST simulation agrees well with the $N = 8$ multipole approximation, independently confirming that multipole approximation are converging to the correct result as the number of poles is increased.

To further test the theoretical framework in this paper, in Figures 12 and 13 we plot the voltage along the line joining the two spheres for the symmetric and anti-symmetric cases for the ratio $a/H = 0.4$.

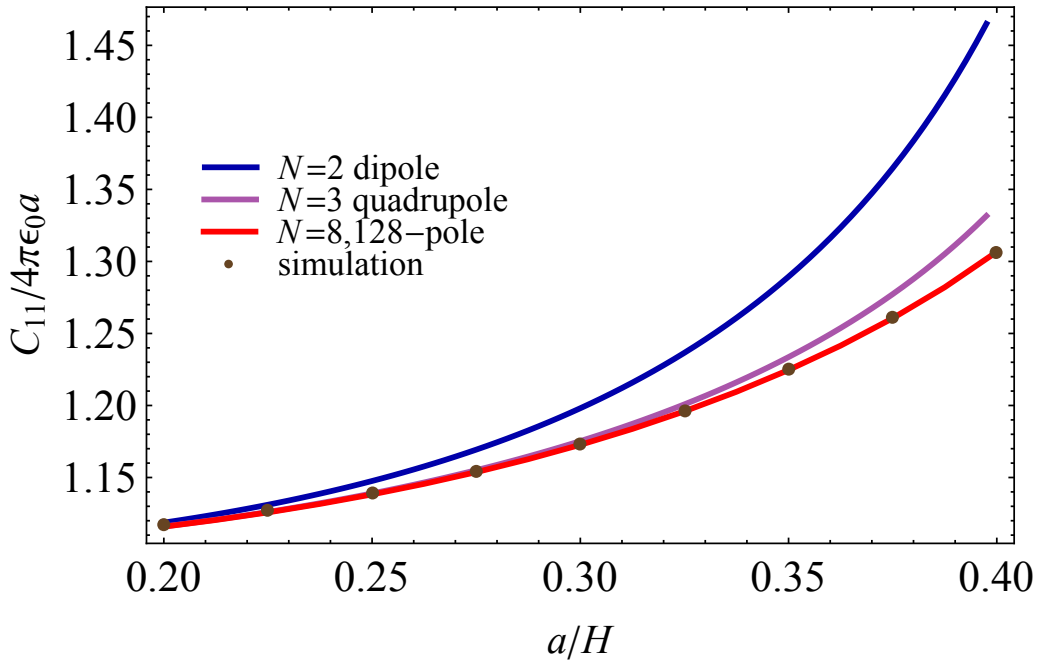

Figure 8: The capacitance coefficient $C_{11}/4\pi\epsilon_0 a$ is plotted versus a/H for $a/R = 0.1$. The dipole (blue), quadrupole (purple), and $N = 8$ (red) are approximations are shown along with simulation (brown dots). The analytical results show convergence and agreement with simulation.

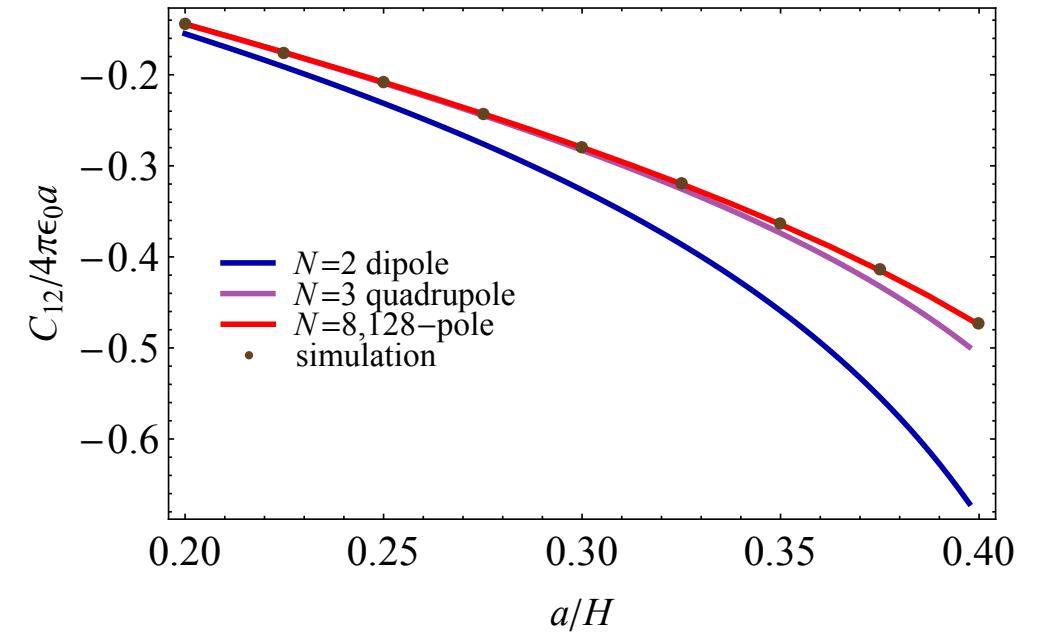

Figure 9: The capacitance coefficient $C_{12}/4\pi\epsilon_0 a$ is plotted versus a/H for $a/R = 0.1$. The dipole (blue), quadrupole (purple), and $N = 8$ (red) are approximations are shown along with simulation (brown dots). The analytical results show convergence and agreement with simulation.

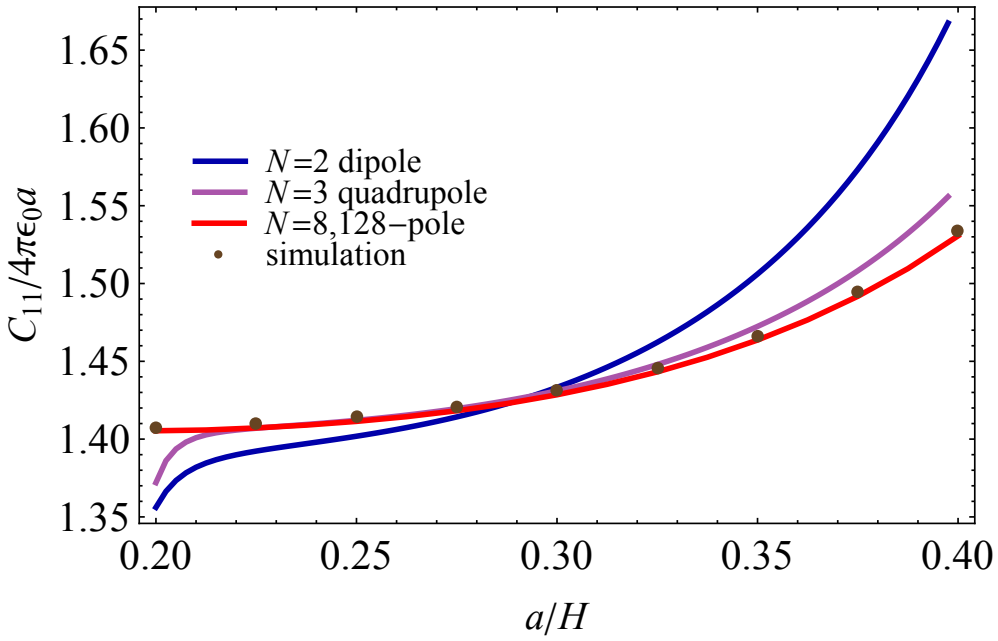

Figure 10: The capacitance coefficient $C_{11}/4\pi\epsilon_0 a$ is plotted versus a/H for $a/R = 0.33$. The dipole (blue), quadrupole (purple), and $N = 8$ (red) are approximations are shown along with simulation (brown dots). The analytical results show convergence and agreement with simulation.

The comparison of the analytical and numerical calculation is seen to be excellent for the potential as well. The agreement is to within 0.1% at all points. The agreement for the symmetric case appears to be a little worse than the anti-symmetric case but that is mainly due to the smaller scale in the symmetric case.

10 Summary

In this paper we calculate the capacitance coefficients of two spheres inside a grounded cylinder in terms of the geometrical parameters a, H and R as shown in Figure 2. We present closed-form analytical results for the capacitances in three different approximations. The monopole approximation in Section 5 is algebraically the simplest and the least accurate of the three. The quadrupole approximation in Section 7 is the most accurate but algebraically the most complex. The dipole approximation lies in between the two in both complexity and accuracy.

For the design of compact Marx generators, that motivated this study, of particular interest are the capacitance coefficients given by Equations (50, 51) in combination with the corresponding monopole terms in the quadrupole approximation, Equations (39) and (42). These results give the capacitances accurately to within a few percent in the parameter space in a/R and H/R explored in the paper. The remainder error plots in Figures 6 and 7 may be used to further improve the calculations. The general formulation presented in Section 4 can be used to obtain arbitrarily accurate results by increasing the number of multipoles used in the approximation provided the parameters are within the range $2a < H \lesssim R$.

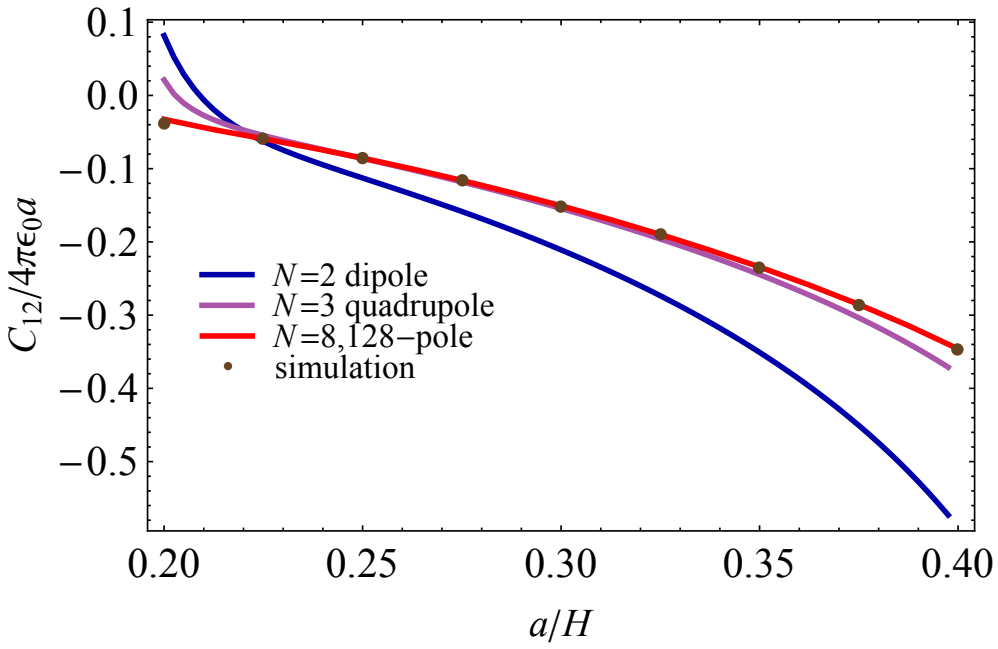

Figure 11: The capacitance coefficient $C_{12}/4\pi\epsilon_0 a$ is plotted versus a/H for $a/R = 0.33$. The dipole (blue), quadrupole (purple), and $N = 8$ (red) are approximations are shown along with simulation (brown dots). The analytical results show convergence and agreement with simulation.

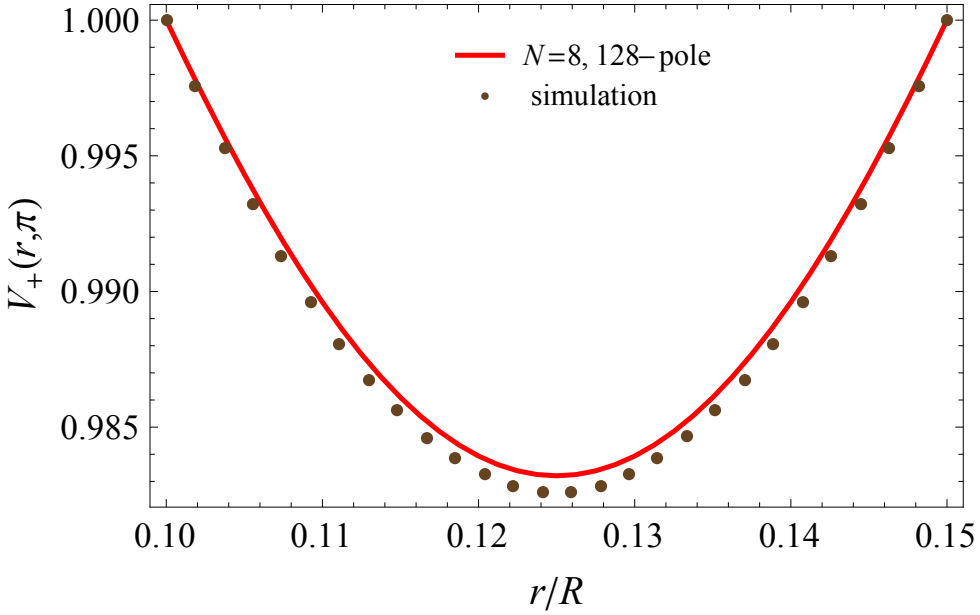

Figure 12: Comparison of the analytical and numerical results of the potential along the line joining the two spheres for $a/H = 0.4$ (symmetric case) shows agreement within a fraction of a percent at all points.

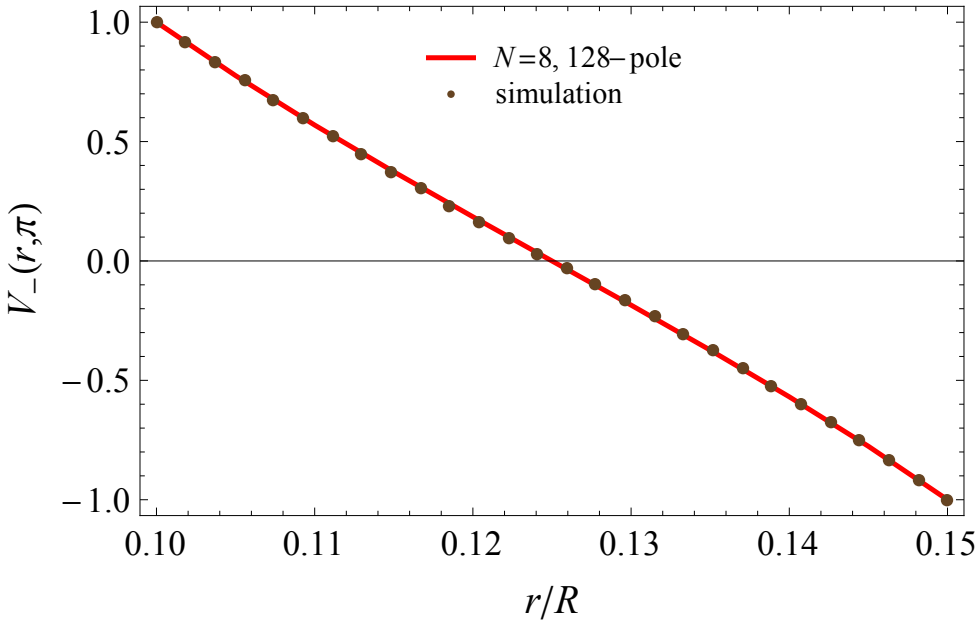

Figure 13: Comparison of the analytical and numerical results of the potential along the line joining the two spheres for $a/H = 0.4$ (anti-symmetric case) shows even better agreement because the potential must pass through zero at the midpoint between the spheres for both plots.

References

[1] D.V. Giri and S. Banerjee, Electrostatic Characteristics of Two Conducting Spheres in a Grounded Cylinder,IEEE Transactions on Plasma Science, Volume 47, Number 8, August 2019, pp 4076 - 4083.

[2] J.C. Pouncey, J.M. Lehr and D.V. Giri, Triggering of Compact Marx Generators, Presented at AMEREM 2018 held at University of Santa Barbara, August 2018.

[3] R.C. Knight, The Potential of a Sphere inside an Infinite Circular Cylinder, Quarterly Journal of Mathematics, Oxford University Press, November 1935.

[4] W.R. Smythe, Charged Sphere in a Cylinder, Journal of Applied Physics, Volume 31, Number 3, March 1960, pp 553–556.

[5] W.R. Smythe, Charged Spheroid in a Cylinder, Journal of Mathematical Physics, Volume 4, Number 6, June 1963, pp 833–837.

[6] I.C. Chang and I.D. Chang, Potential of a Charged Sphere inside a Grounded Cylindrical Tube, Studies in Applied Mathematics, Volume 47, Issue 1-4 , 1967, pp 360–367.

[7] E. Pisler and T. Adhikari, Numerical Calculation of Mutual Capacitance between Two Equal Metal Spheres, Physica Scripta, Volume 2, 1970, pp 81–83 C.

[8] A. Morrison, Potential and Electric Fields of a Conducting Sphere in the Presence of a Charged Conducting Plane, Harry Diamond Laboratories, Adelphi, MD., U. S. Army, HDL Report Number, HDL-TR-2161, Approved for Public Release, Distribution Unlimited, August-Nov 1988

[9] S. Banerjee, M. Levy, M. Davis and B. Wilkerson, Exact and Approximate Capacitance and Force Expressions for the Electrostatic Interaction Between Two Equal-Sized Charged Conducting Spheres, IEEE Transactions on Industry Applications, Volume 53, Number 3, May-June 2017, pp 2455–2460.